

# The effect of $^{60}\text{Co}$ ( $\gamma$ -ray) irradiation on the electrical characteristics of $\text{Au}/\text{SnO}_2/\text{n-Si}$ (MIS) structures

M. Gökçen, A. Tataroğlu\*, Ş. Altındal, M.M. Bülbül

*Physics Department, Faculty of Arts and Sciences, Gazi University, 06500 Teknikokullar, Ankara, Turkey*

Received 18 November 2006; accepted 11 February 2007

## Abstract

The effect of  $^{60}\text{Co}$  ( $\gamma$ -ray) irradiation on the electrical properties of  $\text{Au}/\text{SnO}_2/\text{n-Si}$  (MIS) structures has been investigated using the capacitance–voltage ( $C-V$ ) and conductance–voltage ( $G/\omega-V$ ) measurements in the frequency range 1 kHz to 1 MHz at room temperature. The MIS structures were exposed to  $\gamma$ -rays at a dose rate of 2.12 kGy/h in water and the range of total dose was 0–500 kGy. It was found that the  $C-V$  and  $G/\omega-V$  curves were strongly influenced with both frequency and the presence of the dominant radiation-induced defects, and the series resistance was increased with increasing dose. Also, the radiation-induced threshold voltage shift ( $\Delta V_T$ ) strongly depended on radiation dose and frequency, and the density of interface states  $N_{ss}$  by Hill–Coleman method decreases with increasing radiation dose.

© 2007 Elsevier Ltd. All rights reserved.

PACS: 61.80.Ed; 73.40.Qv; 61.80.-x; 84.37.+q; 77.22.-d

Keywords: Gamma-rays; MIS structure; Radiation effects; Series resistance

## 1. Introduction

MIS structures consist of semiconductor substrate covered by an insulator layer upon which a metal electrode is deposited. The presence of insulating interface layer makes them rather sensitive to irradiation. It is known that energetic  $^{60}\text{Co}$   $\gamma$ -ray irradiation can generate electronic surface states at the semiconductor–insulator (such as  $\text{Si-SnO}_2$  or  $\text{Si-SiO}_2$ ) interface in MIS structures. Exposure of the MIS structures to  $\gamma$ -rays will cause, by means of the Compton electrons, electron–hole pair generation and changes in the crystal lattice (Chin and Ma, 1983; Ma, 1975; Feteha et al., 2002). When the MIS structures are stressed with an external bias, these electron–hole pairs would be separated by the strong local internal electric field at grain boundaries. Electrons are swept out of the insulator layer quickly by the electric field while the holes slowly and could be trapped by the defects. Recently, the radiation response of MIS devices has been found to

change significantly when these devices are exposed to irradiation stress treatments (Nicollian and Goetzberger, 1965; Zainninger and Holmes-Siedle, 1967; Winokur et al., 1976; Benedetto and Boesch, 1984; Winokur et al., 1984; Da Silva et al., 1987; Schwank et al., 1986; Ma, 1989; Witczak et al., 1992; Candelori et al., 1999; Tataroğlu et al., 2003).

Da Silva et al. (1987) were among the first to make a systematic observation of the after-irradiation behavior of radiation-induced interface states ( $N_{ss}$ ) in MIS devices.

When localized interface states exist at the semiconductor–insulator interface, the device behavior is different from an ideal case. The reason is mainly due to the interruption of the periodic lattice structure at the surface (Nicollian and Goetzberger, 1965; Tataroğlu et al., 2003), surface preparation, and formation of insulator layer and impurity concentration of semiconductor (Hung and Cheng, 1987). This interface states usually cause a bias shift and frequency dispersion in the capacitance–voltage ( $C-V$ ) and conductance–voltage ( $G/\omega-V$ ) curves (Ma, 1975). To determine the interface state density traps, various measurement techniques such as the high-low frequency

\*Corresponding author. Tel.: +90 312 212 6030; fax: +90 312 212 2279.  
E-mail address: [ademt@gazi.edu.tr](mailto:ademt@gazi.edu.tr) (A. Tataroğlu).

capacitance (Castagne and Vapaille, 1971; Kelberlau and Kassing, 1979), quasi-static capacitance (Kuhn, 1970), surface admittance (Kar and Varma, 1985) and conductance techniques have been developed, and among them the more important ones are high–low frequency capacitance and conductance technique (Hung and Cheng, 1987).

The promising physical properties of  $\text{SnO}_2$  thin film and their superior chemical stability have motivated its application in many devices, such as solar cells, gas sensors, catalyses devices, and transparent conducting electrodes (Moreno et al., 1997; Dazhi et al., 1994; Chrisey and Hubler, 1994; Auciello and Engemann, 1993). Even though a lot of works have been done on  $\text{SnO}_2$  thin films, to the best of knowledge, the effect of radiation on  $\text{SnO}_2$  thin films has not been studied.

In this work, we present the effect of  $^{60}\text{Co}$   $\gamma$ -ray irradiation on the electrical characteristics of MIS structures using capacitance–voltage ( $C$ – $V$ ) and conductance–voltage ( $G$ – $V$ ) measurements.

## 2. Experimental details

The metal–insulator–semiconductor ( $\text{Au}/\text{SnO}_2/\text{n-Si}$ ) structures used in this work were fabricated using n-type (P-doped) single crystals silicon wafer with  $\langle 111 \rangle$  surface orientation,  $280\text{ }\mu\text{m}$  thick,  $2''$  diameter and  $4.45\text{ }\Omega\text{cm}$  resistivity. The Si wafer was degreased for 5 min in boiling trichloroethylene, acetone and ethanol consecutively and then etched in: first  $\text{H}_2\text{SO}_4$ ,  $\text{H}_2\text{O}_2$  and 20% HF solution, then  $6\text{HNO}_3$ : $1\text{HF}$ : $35\text{H}_2\text{O}$  and 20% HF solution. Preceding each cleaning step, the wafer was rinsed thoroughly in de-ionized water of  $18\text{ M}\Omega\text{cm}$  resistivity. Immediately after surface cleaning, high purity Au metal (99.999%) with a thickness of  $2500\text{ }\text{\AA}$  was thermally evaporated from the tungsten filament onto the whole back surface of the wafer in liquid nitrogen trapped oil-free ultra-high vacuum system in the pressure of  $1 \times 10^{-6}$  Torr. Sintering the evaporated Au, the ohmic contact was formed under vacuum. Immediately after ohmic contact, a thin layer of  $\text{SnO}_2$  was grown on the Si substrate by spraying a solution consisting of 32.21 wt% of ethyl alcohol ( $\text{C}_2\text{H}_5\text{OH}$ ), 40.35 wt% of de-ionized water ( $\text{H}_2\text{O}$ ) and 27.44 wt% of stannic chloride ( $\text{SnCl}_4 \cdot 5\text{H}_2\text{O}$ ) on the substrate, which was maintained at a constant temperature of  $400^\circ\text{C}$ . The temperature of the substrates was monitored by chromel–alumel thermocouple fixed on top surface of the substrate. The variation of the substrate temperature during spray was maintained within  $\pm 2^\circ\text{C}$  with the help of a temperature controller. The rate of spraying was kept at about  $30\text{ cc/min}$  by controlling the carrier gas flowmeter.  $\text{N}_2$  was used as the carrier gas.  $\text{SnO}_2$  dots were  $4\text{ mm}$  in diameter. After spraying process, circular dots of  $2\text{ mm}$  in diameter and  $2500\text{ }\text{\AA}$  thick Au rectifying contacts were deposited onto the  $\text{SnO}_2$  surface of the wafer through a metal shadow mask in liquid nitrogen trapped oil-free ultra-high vacuum system in the pressure of  $1 \times 10^{-6}$  Torr.

Both the thickness of metal layer and deposition rates were monitored with the help of a digital quartz crystal thickness monitor. The deposition rates were about  $1\text{--}3\text{ }\text{\AA}/\text{s}$ . The interfacial oxide layer thickness was estimated to be about  $17\text{ }\text{\AA}$  from measurement of the oxide capacitance in the strong accumulation region for MIS structure. The capacitance–voltage ( $C$ – $V$ ) and conductance–voltage ( $G/\omega$ – $V$ ) measurements were performed in the dark before and after irradiation at various frequencies ( $1\text{ kHz}$ – $1\text{ MHz}$ ) and various radiation doses ( $0\text{--}500\text{ kGy}$ ). These measurements were made via a computer-controlled HP 4192A LF impedance analyzer at test signal of  $50\text{ mV}$ .

## 3. Results and discussion

### 3.1. Frequency-dependent $C$ – $V$ and $G/\omega$ – $V$ measurements

Although the frequency and irradiated characteristics of one of the diodes, MIS1, was presented in this work,

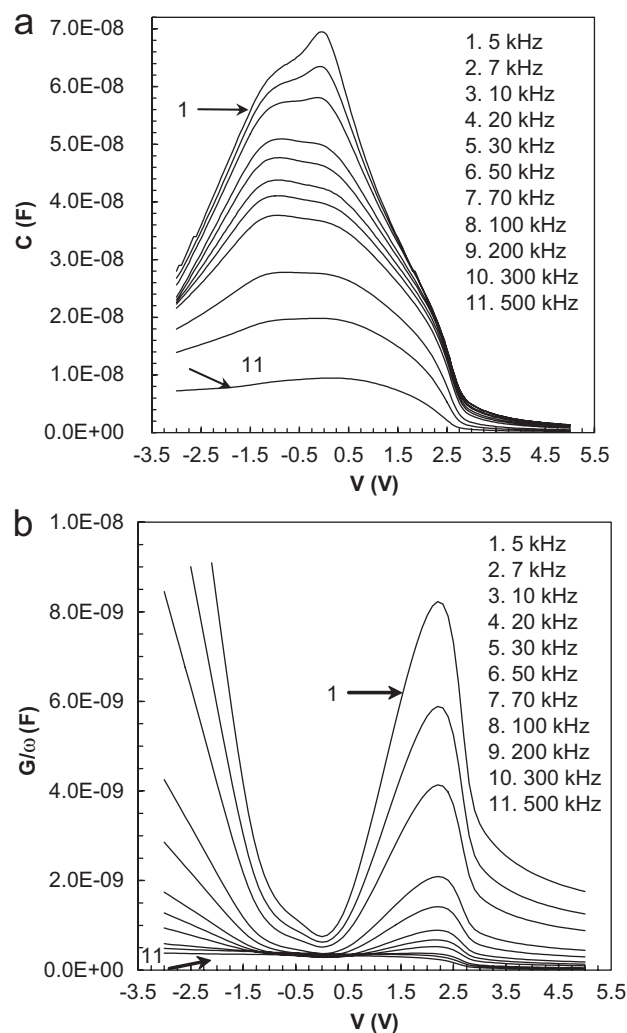


Fig. 1. Capacitance–voltage ( $C$ – $V$ ) and conductance–voltage ( $G/\omega$ – $V$ ) characteristics of  $\text{Au}/\text{SnO}_2/\text{n-Si}$  (MIS1) structure at various frequencies.

other devices fabricated under the same condition showed almost the same characteristics with very similar diode parameters. Fig. 1(a) and (b) shows the measured capacitance–voltage ( $C$ – $V$ ) and conductance–voltage ( $G/\omega$ – $V$ ) characteristics of Au/SnO<sub>2</sub>/n-Si (MIS1) structure for different frequencies, respectively. Both the  $C$ – $V$  and  $G/\omega$ – $V$  characteristics show frequency dispersion. In the depletion and accumulation regions for a given applied voltage,  $C$  and  $G/\omega$  increase with decreasing frequencies due to the time-dependent response of interface states. In addition, each  $C$ – $V$  curve has three regimes of accumulation–depletion–inversion region and gives a peak. The peak position of  $C$  is shifting toward reverse bias region with increasing frequency and almost disappears at high frequencies. This occurs because at lower frequencies the interface states can follow the ac signal and yield an excess capacitance, which depends on the frequency. In the high frequency limit ( $f \geq 500$  kHz), however, the interface states cannot follow the ac signal. This makes the contribution of interface state capacitance to the total capacitance negligibly small (Akkal et al., 2000).

As shown in Fig. 1(b), each  $G$ – $V$  curve clearly shows a distinctive peak at depletion region, further verifying the MIS behaviors of the samples, and also indicating the presence of localized surface states at Si–SnO<sub>2</sub> interfaces. Thus, it can be concluded that under bias ( $V$ ) the interface states are responsible for the observed frequency dispersion in  $C$  ( $V$ ) and  $G$  ( $V$ ) curves. In Fig. 1(b), when the frequency increases from 5 to 500 kHz, the conductance decreases from 0.746 to 0.333 nF at zero bias.

The density of interface states ( $N_{ss}$ ) can be derived from Hill and Coleman (1980) method. According to this method, the density of interface states can be calculated by using the following equation:

$$N_{ss} = \frac{2}{qA} \frac{(G_m/\omega)_{\max}}{((G_m/\omega)_{\max} C_{ox})^2 + (1 - C_m/C_{ox})^2} \quad (1)$$

where  $A$  is the area of the diode,  $\omega$  is the angular frequency,  $(G_m/\omega)_{\max}$  is the maximum measured conductance value.  $C_{ox}$  is the capacitance of insulator layer in strong accumulation region and  $C_m$  is the capacitance value, which corresponding to the  $(G_m/\omega)_{\max}$  value. The values of various parameters for Au/SnO<sub>2</sub>/n-Si MIS structure determined from  $C$ – $V$  and  $G/\omega$ – $V$  characteristics in the frequency range of 5–500 kHz are given in Table 1. As can be seen in Table 1, as the frequency increases further, the peak values of  $C$  and  $G/\omega$  are found to decrease, so do the values of  $N_{ss}$ .

The values of interface state density ( $N_{ss}$ ) are in good agreement with the recent survey (Sze, 1981) on the interface charges where the interface state density ( $N_{ss}$ ) for similarly grown films is between  $1.74 \times 10^{12}$  and  $1.72 \times 10^{11}$  eV<sup>−1</sup> cm<sup>−2</sup>.

The frequency dependency of the series resistance can be obtained from the measurements of  $C$ – $V$ – $f$  and  $G/\omega$ – $V$ – $f$

Table 1

The values of various parameters for Au/SnO<sub>2</sub>/n-Si (MIS1) structure determined from  $C$ – $V$  and  $G/\omega$ – $V$  characteristics in the frequency range of 5–500 kHz

$f$ (kHz)	$V_{\max}$ (V)	$C_m$ (F)	$(G_m/\omega)_{\max}$ (F)	$N_{ss}$ (eV <sup>−1</sup> cm <sup>−2</sup> )
5	2.30	$1.89 \times 10^{-8}$	$8.17 \times 10^{-9}$	$2.27 \times 10^{12}$
7	2.30	$1.94 \times 10^{-8}$	$5.85 \times 10^{-9}$	$1.61 \times 10^{12}$
10	2.30	$1.94 \times 10^{-8}$	$4.10 \times 10^{-9}$	$1.13 \times 10^{12}$
20	2.30	$1.88 \times 10^{-8}$	$2.07 \times 10^{-9}$	$5.77 \times 10^{11}$
30	2.30	$1.85 \times 10^{-8}$	$1.40 \times 10^{-9}$	$3.92 \times 10^{11}$
50	2.30	$1.78 \times 10^{-8}$	$8.82 \times 10^{-10}$	$2.51 \times 10^{11}$
70	2.30	$1.70 \times 10^{-8}$	$6.65 \times 10^{-10}$	$1.92 \times 10^{11}$
100	2.20	$1.58 \times 10^{-8}$	$5.21 \times 10^{-10}$	$1.54 \times 10^{11}$
200	2.30	$1.33 \times 10^{-8}$	$3.49 \times 10^{-10}$	$1.09 \times 10^{11}$
300	2.30	$8.17 \times 10^{-9}$	$2.92 \times 10^{-10}$	$1.00 \times 10^{11}$
500	2.20	$4.22 \times 10^{-9}$	$2.39 \times 10^{-10}$	$8.83 \times 10^{10}$

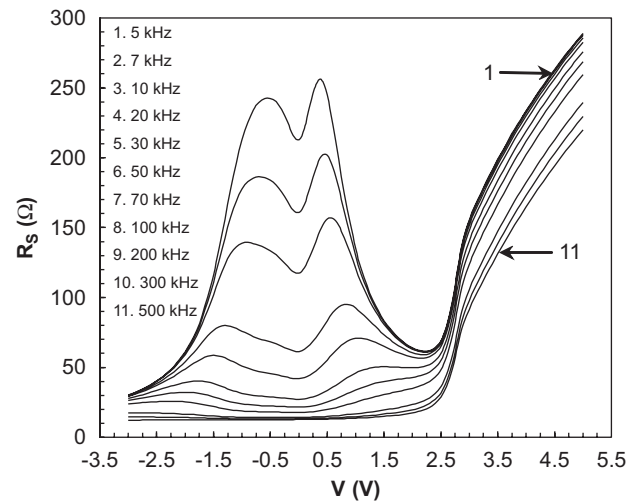


Fig. 2. The variation of the series resistance of Au/SnO<sub>2</sub>/n-Si (MIS1) structure as a function of voltage for various frequencies at room temperature.

curves (Nicollian and Brews, 1982).

$$R_s = \frac{G_m}{G_m^2 + (\omega C_m)^2}, \quad (2)$$

where  $(C_m)$  is measured capacitance and  $(G_m)$  is conductance values in strong accumulation region at high frequency ( $f \geq 500$  kHz). Fig. 2 depicts the voltage dependency of the series resistance for various frequencies. As can clearly seen from the figure, the series resistance gives two peaks in the shape of a hump at about zero bias, decreasing and disappearing with increasing frequencies. Above 2.5 V, the series resistance begins to increase almost linearly. The frequency dependency of series resistance profile versus voltage is similar to the temperature dependence series resistance profile versus voltage (Kar and Narasimhan, 1987). The voltage and frequency dependency of  $R_s$  is attributed to the particular distribution of interface density states and interfacial insulator layer. As a result we can say that at enough high frequencies

( $f \geq 500$  kHz) the interface states cannot follow the ac signal and consequently cannot contribute to the excess capacitance and conductance.

### 3.2. Radiation-dependent $C-V$ and $G/\omega-V$ measurements

Fig. 3(a) and (b) shows the measured capacitance–voltage ( $C-V$ ) and conductance–voltage ( $G/\omega-V$ ) char-

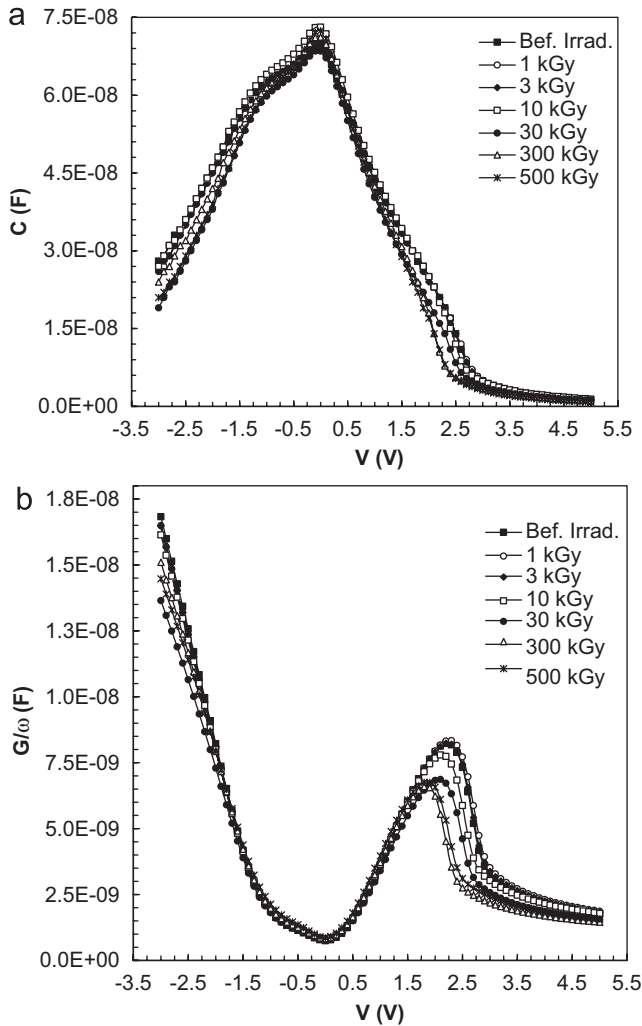


Fig. 3. Capacitance–voltage ( $C-V$ ) and conductance–voltage ( $G/\omega-V$ ) characteristics of Au/SnO<sub>2</sub>/n-Si (MIS1) structure under different doses at 5 kHz.

Table 2

The values of  $N_{ss}$  in the radiation dose range of 0–500 kGy

Irradiation (kGy)	$V_{max}$ (V)	$C_m$ (F)	$(G_m/\omega)_{max}$ (F)	$N_{ss}$ (eV <sup>-1</sup> cm <sup>-2</sup> )
Before irradiation	2.20	$1.89 \times 10^{-8}$	$8.17 \times 10^{-9}$	$2.27 \times 10^{12}$
1	2.30	$1.90 \times 10^{-8}$	$8.33 \times 10^{-9}$	$2.31 \times 10^{12}$
3	2.30	$1.91 \times 10^{-8}$	$8.20 \times 10^{-9}$	$2.27 \times 10^{12}$
10	2.10	$2.30 \times 10^{-8}$	$7.78 \times 10^{-9}$	$1.98 \times 10^{12}$
30	2.10	$1.80 \times 10^{-8}$	$6.85 \times 10^{-9}$	$1.94 \times 10^{12}$
300	1.80	$2.20 \times 10^{-8}$	$6.75 \times 10^{-9}$	$1.76 \times 10^{12}$
500	1.80	$2.40 \times 10^{-8}$	$6.59 \times 10^{-9}$	$1.64 \times 10^{12}$

acteristics of Au/SnO<sub>2</sub>/n-Si (MIS1) structure at room temperature and 5 kHz for test devices irradiated to 1, 3, 10, 30, 300, and 500 kGy.

By irradiation, the  $C-V$  curve moves towards the negative voltage with increasing irradiation dose and the voltage shift  $\Delta V$  changes from 2.0 to 2.4 V with increasing irradiation from 0 to 500 kGy. This shift is due to trapped positive charges in the SnO<sub>2</sub> insulator layer, as reported in the literature (Benedetto and Boesch, 1984; Karimov et al., 2005; Chauhan and Chakrabarti, 2002).

The density of interface states ( $N_{ss}$ ) can be derived from Eq. (1) using the measured capacitance ( $C_m$ ) and conductance values ( $G_m$ ) under radiation (Hill and Coleman, 1980). The values of  $N_{ss}$  in the radiation dose range of 0–500 kGy are given in Table 2. As shown in Table 2, the  $N_{ss}$  slightly decreases with increase in radiation dose. The results of the Au/SnO<sub>2</sub>/n-Si show that they are expected to be useful in predicting the behavior of Au/SnO<sub>2</sub>/n-Si-based devices operating in radiation environment.

The values of series resistance of the sample at strong accumulation region (–3 V) for the device irradiated to 1, 3, 10, 30, 300, and 500 kGy were calculated as 13.28, 13.93, 14, 14.24, 16.10, 18.81, and 22.54 Ω, respectively. In general, as shown in Fig. 4, the series resistance increases with increase in radiation dose. In strong accumulation

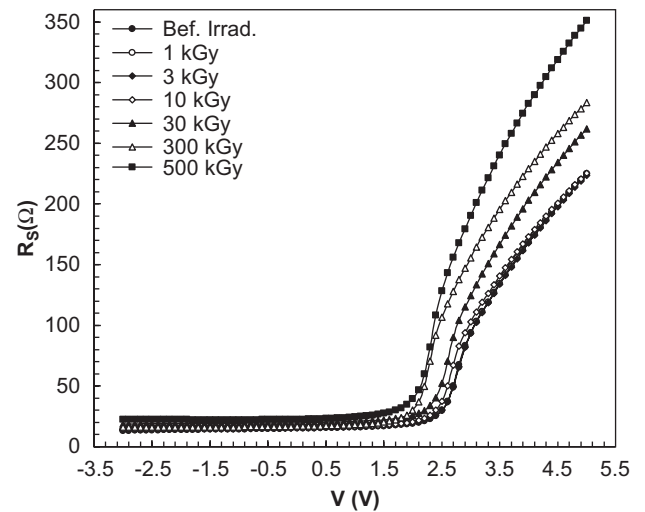


Fig. 4. Radiation dependency of the series resistance of Au/SnO<sub>2</sub>/n-Si (MIS1) structure at room temperature at 5 kHz.

region, it is almost independent of the voltage. However, it steeply increases with voltage and radiation dose in the inversion region. These values of  $R_s$  indicate that special attention should be given to the effects of series resistance in the application of the  $C$ – $V$  and  $G/\omega$ – $V$  measurements.

#### 4. Conclusion

The effect of frequency and  $\gamma$ -ray irradiation on the electrical characteristics of Au/SnO<sub>2</sub>/n-Si Schottky diode has been studied using  $C$ – $V$  and  $G/\omega$ – $V$  measurements. Experimental results show that the capacitance ( $C$ ) and conductance ( $G/\omega$ ) decrease with increasing frequency due to a continuous distribution of  $N_{ss}$  in equilibrium with Si. The series resistance gives two peaks in the shape of a hump at about zero bias, decreasing and disappearing with increasing frequencies. But, above 2.5 V, it begins to increase almost linearly. An increase in capacitance and conductance due to the irradiation-induced defects at the interface has been observed. Also, exposure to increasing cumulative  $\gamma$ -ray doses has the effects: (i) increases in the series resistance  $R_s$  obtained from  $C$ – $V$  and  $G/\omega$ – $V$  measurements and (ii) slightly decrease in the interface states  $N_{ss}$  with increasing radiation dose, indicating high stability in radiation environment.

#### References

- Akkal, B., Benamara, Z., Gruzza, B., Bideux, L., 2000. Characterization of interface states at Au/InSb/InP (100) Schottky barrier diodes as a function of frequency. *Vacuum* 57, 219–238.
- Auciello, O., Engemann, J., 1993. Multicomponent and Multilayered Thin Films for Advanced Microtechnologies: Techniques Fundamentals and Devices. Kluwer, Dordrecht.
- Benedetto, J.M., Boesch Jr., H.E., 1984. MOSFET and MOS capacitor responses to ionizing radiation. *IEEE Trans. Electron. Nucl. Sci.* NS-31 (6), 1461–1466.
- Candelori, A., Paccagnella, A., Cammarata, M., Ghidini, G., Ceschia, M., 1999. Electron irradiation effect on thin MOS capacitors. *J. Non-Cryst. Solids* 245, 238–244.
- Castagne, R., Vapaille, A., 1971. Description of the SiO<sub>2</sub>-Si interface properties by means of very low frequency MOS capacitance measurements. *Surf. Sci.* 28 (1), 157–193.
- Chauhan, R.K., Chakrabarti, P., 2002. Effect of ionizing radiation on MOS capacitors. *Microelectron. J.* 33, 197–203.
- Chin, M.R., Ma, T.P., 1983. Gate-width dependence of radiation-induced interface traps in metal/SiO<sub>2</sub>/Si devices. *Appl. Phys. Lett.* 42 (10), 883–885.
- Chrissey, D.B., Hubler, G.K., 1994. Pulsed Laser Deposition of Thin Films. Wiley, New York.
- Da Silva Jr., E.F., Nishioka, Y., Ma, T.P., 1987. Radiation response of MOS capacitors containing fluorinated oxides. *IEEE Trans. Nucl. Sci.* NS-34 (6), 1190–1195.
- Dazhi, W., Shulin, W., Jun, C., Suyuan, Z., Fangqing, L., 1994. Microstructure of SnO<sub>2</sub>. *Phys. Rev. B* 49, 14282–14285.
- Feteiha, M.Y., Soliman, M., Gomaa, N.G., Ashry, M., 2002. Metal-insulator-semiconductor solar cell under gamma irradiation. *Renewable Energy* 26, 113–120.
- Hill, W.A., Coleman, C.C., 1980. A single frequency approximation for interface state density determination. *Solid-State Electron.* 23 (9), 987–993.
- Hung, K.K., Cheng, Y.C., 1987. Characterization of Si-SiO<sub>2</sub> interface traps in p-metal-oxide-semiconductor structures with thin oxides by conductance technique. *J. Appl. Phys.* 62 (10), 4204–4211.
- Kar, S., Narasimhan, R.L., 1987. Characteristics of the Si-SiO<sub>2</sub> interface states in thin (70–230 Å) oxide structures. *J. Appl. Phys.* 61 (12), 5353–5359.
- Kar, S., Varma, S., 1985. Determination of silicon-silicon dioxide interface state properties from admittance measurements under illumination. *J. Appl. Phys.* 58 (11), 4256–4266.
- Karimov, Kh.S., Ahmed, M.M., Moiz, S.A., Fedorov, M.I., 2005. Temperature-dependent properties of organic-on-inorganic Ag/p-CuPc/n-GaAs/Ag photoelectric cell. *Sol. Energy Mater. Sol. Cells* 87, 61–75.
- Kelberlau, U., Kassing, R., 1979. Theory of nonequilibrium properties of MIS capacitors including charge exchange of interface states with both bands. *Solid-State Electron.* 22 (1), 37–45.
- Kuhn, M., 1970. A quasi-static technique for MOS  $C$ – $V$  and surface state measurements. *Solid-State Electron.* 13 (6), 873–885.
- Ma, T.P., 1975. Oxide thickness dependence of electron-induced surface states in MOS structures. *Appl. Phys. Lett.* 27 (11), 615–617.
- Ma, T.P., 1989. Interface trap transformation in radiation or hot-electron damaged MOS structures. *Semicond. Sci. Technol.* 4, 1061–1079.
- Moreno, M.S., Varela, A., OteroDiaz, L.C., 1997. Cation nonstoichiometry in thin-monoxide-phase Sn<sub>1-delta</sub>O with tweed microstructure. *Phys. Rev. B* 56, 5186–5192.
- Nicollian, E.H., Brews, J.R., 1982. *MOS Physics and Technology*. Wiley, New York.
- Nicollian, E.H., Goetzberger, A., 1965. MOS conductance technique for measuring surface state parameters. *Appl. Phys. Lett.* 7, 216–219.
- Schwank, J.R., Winokur, P.S., Sexton, F.W., Fleetwood, D.M., Perry, J.H., Dressendorfer, P.V., Sanders, D.T., Turpin, D.C., 1986. Radiation-induced interface-state generation in MOS devices. *IEEE Trans. Nucl. Sci.* NS-33 (6), 1178–1184.
- Sze, S.M., 1981. *Physics of Semiconductor Devices*, second ed. Wiley, New York.
- Tataroğlu, A., Altındal, Ş., Karadeniz, S., Tuğluoğlu, N., 2003. Au/SnO<sub>2</sub>/n-Si (MOS) structures response to radiation and frequency. *Microelectron. J.* 34, 1043–1049.
- Zaininger, K.H., Holmes-Siedle, A.G., 1967. A survey of radiation effect in metal-insulator-semiconductor devices. *RCA Rev.*, 208–239.
- Winokur, P.S., McGarrity, J.M., Boesch, H.E., 1976. Dependence of interface-state buildup on hole generation and transport in irradiated MOS capacitors. *IEEE Trans. Nucl. Sci.* NS-23, 1580–1585.
- Winokur, P.S., Schwank, J.R., McWhorter, P.J., Dressendorfer, P.V., Turpin, D.C., 1984. Correlating the radiation response of MOS capacitors and transistors. *IEEE Trans. Nucl. Sci.* NS-31, 1453–1460.
- Witzak, S.C., Suehle, J.S., Gaitan, M., 1992. An experimental comparison of measurement techniques to extract Si-SiO<sub>2</sub> interface trap density. *Solid-State Electron.* 35 (3), 345–355.